



# CHORUS

This is the accepted manuscript made available via CHORUS. The article has been published as:

## Field Theory of Charge Sharpening in Symmetric Monitored Quantum Circuits

Fergus Barratt, Utkarsh Agrawal, Sarang Gopalakrishnan, David A. Huse, Romain Vasseur, and Andrew C. Potter

Phys. Rev. Lett. **129**, 120604 — Published 13 September 2022

DOI: [10.1103/PhysRevLett.129.120604](https://doi.org/10.1103/PhysRevLett.129.120604)

# Field theory of charge sharpening in symmetric monitored quantum circuits

Fergus Barratt,<sup>1</sup> Utkarsh Agrawal,<sup>1</sup> Sarang Gopalakrishnan,<sup>2</sup>  
David A. Huse,<sup>3,4</sup> Romain Vasseur,<sup>1</sup> and Andrew C. Potter<sup>5</sup>

<sup>1</sup>*Department of Physics, University of Massachusetts, Amherst, MA 01003, USA*

<sup>2</sup>*Department of Physics, The Pennsylvania State University, University Park, PA 16802, USA*

<sup>3</sup>*Department of Physics, Princeton University, Princeton NJ 08544, USA*

<sup>4</sup>*Institute for Advanced Study, Princeton NJ 08540, USA*

<sup>5</sup>*Department of Physics and Astronomy, and Quantum Matter Institute, University of British Columbia, Vancouver, BC, Canada V6T 1Z1*

Monitored quantum circuits (MRCs) exhibit a measurement-induced phase transition between area-law and volume-law entanglement scaling. MRCs with a conserved charge additionally exhibit two distinct volume-law entangled phases that cannot be characterized by equilibrium notions of symmetry-breaking or topological order, but rather by the non-equilibrium dynamics and steady-state distribution of charge fluctuations. These include a charge-fuzzy phase in which charge information is rapidly scrambled leading to slowly decaying spatial fluctuations of charge in the steady state, and a charge-sharp phase in which measurements collapse quantum fluctuations of charge without destroying the volume-law entanglement of neutral degrees of freedom. By taking a continuous-time, weak-measurement limit, we construct a controlled replica field theory description of these phases and their intervening charge-sharpening transition in one spatial dimension. We find that the charge fuzzy phase is a critical phase with continuously evolving critical exponents that terminates in a modified Kosterlitz-Thouless transition to the short-range correlated charge-sharp phase. We numerically corroborate these scaling predictions also hold for discrete-time projective-measurement circuit models using large-scale matrix-product state simulations, and discuss generalizations to higher dimensions.

**Introduction** – Understanding the role of environmental dissipation and decoherence in large quantum circuits is essential for understanding the fundamental capabilities and limitations of noisy quantum computation relevant for near-term devices. A key conjecture of quantum complexity theory is that the output of individual quantum circuits is quite generally exponentially-hard (in qubit number) to predict classically. Examples where a full microscopic descriptions are intractable abound in physical systems: from tracking individual motion of thermodynamically-many colliding gas particles, to computing the complex level structure of chaotic nuclei. Here, the successful philosophy of statistical mechanics and random matrix theory has taught us that the statistical properties of *ensembles* of such complex systems can be far simpler to describe than individual realizations, and in many cases exhibit beautifully universal, model-independent properties.

This observation has motivated the search for an analogous statistical mechanics paradigm for ensembles of random quantum circuits [1–8]. For circuits with ideal (noiseless) gates, this has led to identification of universal features of entanglement growth [8, 9], scrambling [8, 10–12], and quantum chaos [13–18]. Further, exploring monitored random circuits (MRCs), where decoherence is modeled by random measurements of the system by its environment, has revealed the possibility of sharp measurement-induced phase transitions (MIPTs) [19, 20] in the quantum trajectories (i.e. states produced by an MRC for fixed measurement outcomes) between a scrambling regime dominated by unitary gate evolution, and purifying dynamics dominated by measurement induced

collapse [19–62]. These raise the intriguing prospect of using statistical mechanics tools [28, 29, 63, 64] to study quantum communication channel capacity [25, 65], error-correction thresholds [25, 27, 43, 45, 57], and computational complexity [66, 67]. Finite-size evidence for such entanglement MIPT was even recently observed experimentally in trapped-ion chains [68].

In physical systems, symmetries play a central role in determining universal properties of phase transitions and protecting stable and distinct phases of matter, and may be naturally expected to play an important role in measurement-induced phases and critical phenomena in MRCs. Indeed, there is accumulating numerical evidence that symmetries can give rise to multiple distinct phases and critical phenomena in the highly-entangled regime – which would support only classical, incoherent orders in thermal equilibrium. To date, the study of such measurement-stabilized orders has largely resorted to numerical analyses on Clifford circuits [33–35, 52]. Here, building on a statistical mechanics mapping developed in Ref. [56], we construct a replica field-theory framework to analytically study phases and critical phenomena in the volume-entangled regime of MRCs. We focus on the application of this technique to studying charge-sharpening transitions in more generic  $1d$  MRCs with a conserved  $U(1)$  charge or spin, and show that this transition is captured by a modified Kosterlitz-Thouless transition, and validate this prediction against large-scale matrix-product state (MPS) numerics.

**Model of random circuits with symmetries** – We consider a model [11] consisting of a  $1d$  lattice, with a charged qubit with charge-basis states  $|q = \pm 1\rangle$  and a

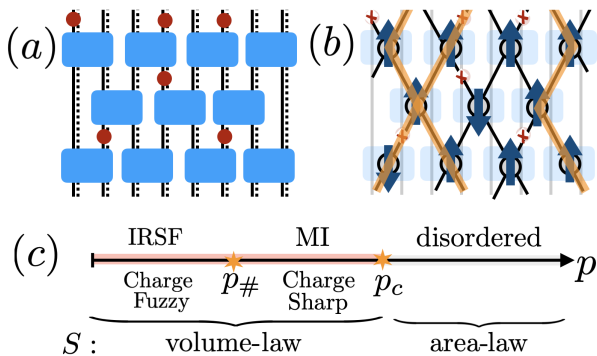


FIG. 1. **Model and phase diagram** – (a) Monitored random circuit (MRC) with charged qubits (solid lines) and neutral large- $d$  qudits (dashed lines) interacting with Haar-random gates (blue boxes) and randomly placed measurements (red dots). (b) Statistical mechanics (stat-mech) model for replicated MRC consists of replica permutation “spins” (arrows) interacting with random-walking charge world-lines (orange lines). (c) The phase diagram, with phases labeled in the MRC (bottom) and stat-mech (top) language respectively. In addition to the entanglement transition at  $p_c$ , which corresponds to a (dis)ordering transition of the permutation “spins”, there is a charge-sharpening transition in the volume law phase, corresponding to an inter-replica superfluid (IRSF) to Mott-insulator (MI) transition in the statistical mechanics language. In  $1+1d$ , this charge sharpening transition has a modified Kosterlitz-Thouless universality class, and the IRSF is a critical/Goldstone phase with scaling exponents that vary continuously with  $p$ .

neutral  $d$ -level qudit on each site, that evolves under a “brick wall” circuit of nearest-neighbor gates that conserve the total charge of the qubit pair, but are otherwise Haar-random in each block of fixed total charge. We consider randomly-placed single-site projective measurements with probability  $p$ . These measurements occur in the charge basis of the qubits and an arbitrary basis of the qudits. As shown in Ref. [56], this model supports two types of phase transitions (separating three distinct dynamical phases): an area-to-volume law entanglement transition at  $p = p_c$  (identical to that of asymmetric circuits), and a “charge-sharpening” transition at  $p = p_\#$  occurring within the volume-law entangled phases. The charge-sharpening transition distinguishes a charge-fuzzy phase ( $p < p_\#$ ) in which scrambling is able to “hide” quantum superpositions of total charge from the measurements for a time that diverges with the system size, and a charge-sharp phase ( $p > p_\#$ ) in which the measurements collapse quantum superpositions of different total charge at a finite-rate. Throughout both phases the neutral qudit (and the charged qubit) degrees of freedom remain volume-law entangled.

As shown in Ref. 56, the statistical properties of entanglement and charge correlators for this MRC ensemble can be captured, via a replica trick, by a classical statistical mechanics model defined on the graph of the quantum circuit (i.e. identifying gates with vertices and qubit

world-lines between gates with links), and consisting of the following degrees of freedom: i) replica permutation “spins”  $s_i \in S_Q$  on each vertex  $i$  where  $Q$  is the number of replica copies, and ii) charge degrees of freedom  $q_{\ell,a} \in \{\pm 1\}$  on each link  $\ell$  and replica  $a = 1 \dots Q$ . As previously described in multiple works [28, 29, 63, 64] the entanglement transition at  $p_c$  appears as an order/disorder transition of the permutation spins.

Here, we focus on the charge-sharpening transition that occurs in the volume-law phase where the permutation spins remain ordered, and can be traced out to obtain a description purely in terms of the charge degrees of freedom. This can be done exactly in the limit of large qudit dimension  $d$ . Further, since the permutation degrees of freedom are gapped for  $p = p_\# < p_c$ , we finite  $d$  corrections will only renormalize the parameters of the effective field theory without altering the universal scaling properties. The resulting charge dynamics are then described by a classical stochastic process in each replica. Measurements force the charges to coincide across replicas at the measured link, creating a space-time-disordered inter-replica interaction.

These charge dynamics are described by a stochastic Markov process for the diagonal components of the (replicated) density matrix in the charge basis (with off-diagonal coherences strictly vanishing due to the qudit “baths”). These form a  $2^{LQ}$  component vector:  $|\rho_Q\rangle$ , which, if correctly normalized, satisfies  $\langle 1|\rho_Q\rangle = \text{tr}\hat{\rho}_Q = 1$  where  $|1\rangle$  is the vector with all unit entries. The measurement- and gate- averaged evolution is described by a transfer matrix:

$$|\rho_Q(t+1)\rangle = T_{\vec{m}(t+1/2)} T_{U,o} T_{\vec{m}(t)} T_{U,e} |\rho_Q(t)\rangle, \quad (1)$$

where  $T_{U,e/o} = \prod_{\langle ij \rangle \in e/o} \prod_{a=1}^Q \frac{1}{4} (\vec{\sigma}_{a,i} \cdot \vec{\sigma}_{a,j} + 3)$  project onto the spin-triplet sector for each bond and represent the evolution from random gates on even(e)/odd(o) bonds, and  $\vec{\sigma}$  are Pauli matrices with  $\sigma_{a,i}^z$  eigenvalue corresponding to the charge at link  $i \in \{1 \dots L\}$  in replica  $a \in \{1 \dots Q\}$ . The measurement operators:  $T_{\vec{m}(t)} = \prod_{i \in \mathcal{M}(t)} \prod_{a=1}^Q \delta_{\sigma_{a,i}^z, m_i(t)}$  simply force the charges in all replicas to agree with the measurement outcomes  $\vec{m}(t)$  on measured links  $\mathcal{M}(t)$  at time-slice  $t$ .

In the following, we will not work with explicitly normalized states, and use the replica trick to properly compute moments of local observables as:

$$\begin{aligned} \mathbb{E} \left[ \langle \hat{O}_1 \rangle \langle \hat{O}_2 \rangle \right] &= \mathbb{E} \left[ \frac{\langle 1|O_1^{(d)}|\rho_1\rangle \langle 1|O_2^{(d)}|\rho_1\rangle}{\langle 1|\rho_1\rangle^2} \langle 1|\rho_1\rangle \right] \\ &= \lim_{Q \rightarrow 1} \langle 1|O_1^{(d)} \otimes O_2^{(d)} \otimes \mathbb{1} \dots \otimes \mathbb{1} |\mathbb{E}[\rho_Q]\rangle, \quad (2) \end{aligned}$$

where  $\mathbb{E}[\dots]$  denotes an average over trajectories, and  $\langle \dots \rangle$  denotes the quantum average within a trajectory, and we define the diagonal part of a quantum operator  $\hat{O}$  as  $O^{(d)} = \sum_m \langle m|\hat{O}|m\rangle |m\rangle \langle m|$  where  $|n\rangle$  is a basis state with definite  $\hat{\sigma}_{a,i}^z = m_{a,i}$ . In the first line, the factors

of  $\langle 1|\rho\rangle$  in the denominator serve to explicitly normalize the state, and the extra factor of  $\langle 1|\rho\rangle$  in the numerator weights each measurement outcome by its Born probability.

In Ref. [56], this transfer-matrix model was analyzed explicitly using exact diagonalization (ED) methods. Here, we benchmark the field-theory predictions representing  $|\rho\rangle$  as a matrix product state (MPS) using time-evolving block decimation (TEBD) analysis of Eq. 1 [69–71]. We emphasize that in this statistical mechanics-description, the volume law phases of the physical qubits correspond to area-law (with log-violation for  $p < p\#$ ) phases of the statistical mechanics “spins”,  $\vec{\sigma}$ , enabling us to obtain results on much larger systems than ED (up to  $\approx 60$  sites <sup>1</sup>).

**Effective field theory** – To gain an analytic handle on the charge dynamics, define a continuous time version of the stroboscopic/circuit evolution of Eq. 1, by replacing the spin-triplet projectors in the  $T_U$  terms with a ferromagnetic interaction  $\frac{1}{4}(\vec{\sigma}_i \cdot \vec{\sigma}_j + 3) \rightarrow e^{J\vec{\sigma}_i \cdot \vec{\sigma}_j dt}$ , and replacing sharp projective measurements in  $T_{\bar{m}}$  by Gaussian-softened “weak” measurements:  $\delta_{\sigma_{a,i}^z, m_i(t)} \rightarrow \exp\left[-\frac{\gamma}{2}\sum_a(\sigma_{a,i}^z - m_i(t))^2\right]$ , where  $J$  and  $\gamma$  are now treated as adjustable parameters that respectively control the strength of unitary gate evolution and measurements respectively. We note that a similar strategy was used in [52] to study  $\mathbb{Z}_2$ -symmetric circuits with  $Q = 2$  replicas. However working at specific replica number is known to give (sometimes even qualitatively) wrong predictions of phases and critical properties. Here, we will use the large- $d$  qudits to take the proper replica limit and recover exact scaling results. We further argue that the universal results of this approach are actually exact for finite  $d$ .

Averaging over measurement outcomes, the transfer matrix for time  $t$  then takes the form of imaginary time with respect to a lattice Hamiltonian:  $T(t) = e^{-tH}$  with:

$$H = -J \sum_{\langle i,j \rangle; a} \vec{\sigma}_{a,i} \cdot \vec{\sigma}_{a,j} + \frac{\gamma}{2} \sum_{i;a,b} \sigma_{a,i}^z \Pi_{ab} \sigma_{b,i}^z, \quad (3)$$

where  $\Pi_{ab} = \left(\delta_{ab} - \frac{1}{Q}\right)$  is a projector onto replica-asymmetric modes.

Without measurements ( $\gamma = 0$ ), the random circuit dynamics simply takes the form of imaginary time evolution with  $SU(2)$  invariant Heisenberg ferromagnet dynamics. The long-time steady states (ground-states of  $H$ ) are simply equal weight superpositions over all charge configurations with each fixed total charge. The elementary excitations of  $H_{\gamma=0}$  (corresponding to decaying perturbations to the steady-state) are magnon excitations with

dispersion (wave-vector dependent decay rate)  $\varepsilon_k \sim Jk^2$ . These simply reflect the diffusive relaxation dynamics of conserved charges. Measurements penalize differences in  $\sigma^z$  between different replicas. After averaging over the space-time quenched disorder due to measurement locations and outcomes, this introduces inter-replica interactions and produces an easy-plane anisotropy for the inter-replica modes (i.e. fluctuations that are different in different replicas, and do not contribute to the average over replicas, see below for precise definitions).

We next construct an effective field theory by writing  $T(t)$  as a spin-coherent state path integral in terms of polar angles  $\theta_{i,a}$  and azimuthal angles  $\phi_{i,a}$  for each spin [72]. For specificity, we work near zero charge density  $\theta = \pi/2 + \delta\theta$ . Integrating out all  $(Q-1)$  components of the out-of-plane fluctuations in the inter-replica modes,  $\Pi\theta$ , which are massive for any  $\gamma > 0$ , and performing a fluctuation and gradient expansion gives an effective action  $\langle 1|T(t)|\rho_Q\rangle = \mathcal{Z}_Q = \int D[\theta, \phi] e^{-\int_0^t dt \int dx \mathcal{L}_{\text{eff}}}$  with:

$$\mathcal{L}_{\text{eff}} = \frac{i}{2} \delta\bar{\theta} \partial_t \bar{\phi} + \frac{\bar{\rho}}{2} \left[ (\partial_x \delta\bar{\theta})^2 + (\partial_x \bar{\phi})^2 \right] + \frac{\rho_s}{2} (\partial_\mu \Pi\phi)^2, \quad (4)$$

where  $\mu \in \{t, x\}$ , and repeated indices are implicitly summed,  $\bar{\rho} \sim J$ ,  $\rho_s \sim \sqrt{J/\gamma}$ , and we have defined the replica average modes:  $\bar{\phi}, \bar{\theta} \equiv \frac{1}{Q} \sum_{a=1}^Q \phi_a, \theta_a$  <sup>3</sup>. To compute correlators as in Eq. 2, this action should be supplemented by boundary conditions corresponding to the final state  $\langle 1|$  which is an equal weight superposition of all charge states, corresponding to a product state of spins point along the  $\hat{x}$  direction:  $(\theta, \phi) = (\frac{\pi}{2}, 0)$  at the final time,  $t$ . In particular, steady-state ( $t \sim L \rightarrow \infty$ ) correlators are generated from the partition function on the half-plane  $(t, x) \in (-\infty, 0] \times \mathbb{R}$  with boundary conditions  $\phi_a(t=0, x) = 0$  and appropriate (charge-diagonal) operators inserted. As a consequence, steady-state properties of MIPTs will correspond to *boundary-critical properties* of the statistical mechanics problem.

The “replica-average” modes  $\bar{\phi}$  determine simple linear observable averages,  $\bar{O} = \mathbb{E}[\langle \bar{O} \rangle]$ . These are unaffected by measurements and have a simple FM spin-wave action and converge to  $\text{tr } \hat{O}$  at late times independent of  $\gamma$ . This accords with the well-known fact that MIPTs are only visible in higher-moments and non-linear functions of state.

The inter-replica fluctuations,  $\Pi\phi$ , control disconnected moments of correlation functions such as  $\mathbb{E}[\langle O(x)O(0) \rangle - \langle O(x) \rangle \langle O(0) \rangle]$ . When singular vortex

<sup>1</sup> While much larger critical systems with 100’s or 1000’s of sites can be simulated by MPS methods in clean 1d systems, here, the disordered nature of the model adds significant sampling complexity and limits the achievable system size.

<sup>2</sup> We note that this expression is approximate: this quantity is non-universal and can be renormalized by irrelevant perturbations neglected in our derivations.

<sup>3</sup> More generally,  $\rho_s$  depends on the space-time local charge density. But this coupling is RG-irrelevant in 1+1d so we drop it here, although it can become relevant in higher  $d$ , as we discuss later.

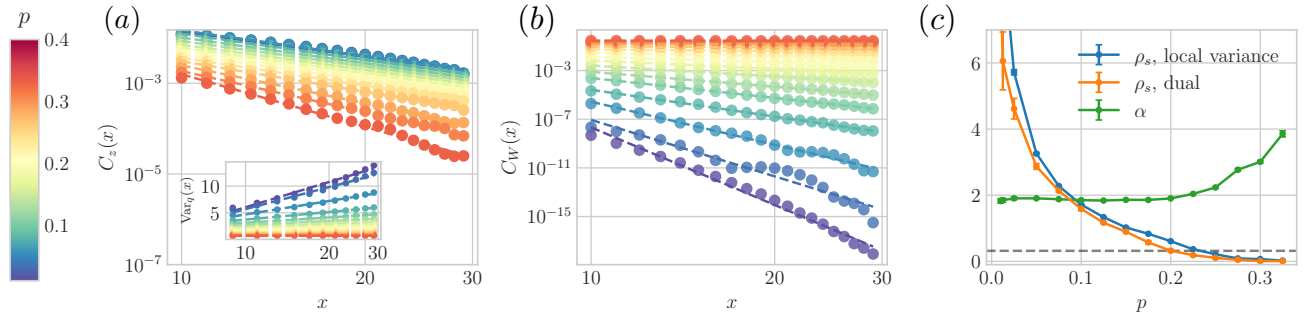


FIG. 2. **TEBD data** – (a) Charge fluctuations  $C_z(x) = \mathbb{E}[\langle \sigma_x^z \sigma_0^z \rangle - \langle \sigma_x^z \rangle \langle \sigma_0^z \rangle]$ , scaling as  $C_z(x) \sim x^{-\alpha}$  in the fuzzy phase. Inset: charge variance of an interval of size  $x$ ,  $\text{Var}_q(x) = \sum_{0 < i, j < x} \mathbb{E}[\langle \sigma_i^z \sigma_j^z \rangle_c]$ , predicted to scale as  $\sim \frac{8\rho_s}{\pi} \log x$ . (b) Dual string disorder parameter  $C_W(x) = \mathbb{E}[\langle W_{[0,x]} \rangle^2]$  with  $W_{[0,x]} = \prod_{0 < i < x} \sigma_i^z$ , showing power-law decay  $C_W(x) \sim x^{-2\pi\rho_s}$  in the charge-fuzzy phase. (c) Continuously evolving superfluid density  $\rho_s$  as a function of  $p$ , extracted from the local charge variance (blue) and the dual correlator  $C_W(x)$  (orange). The dashed horizontal line indicates the critical threshold  $(\rho_s)_\# = \pi^{-1}$ . For  $p < p_\# \sim 0.2$ , the charge correlator  $C_z(x)$  decays with an exponent  $\alpha = 2$  (green).

configurations in the phase-fields are irrelevant ( $0 < \gamma < \gamma_\#$ ) the inter-replica modes follow a superfluid action with  $(Q - 1)$  decoupled relativistic Goldstone-mode excitations which indicate that charge fluctuations with wave-vector  $k$  decay at rate  $\sim |k|$  (dynamical exponent  $z = 1$ ). This inter-replica-superfluid (IRSF) phase represents the charge-fuzzy phase ( $0 < p \leq p_\#$  in the circuit model). Since the effective “superfluid stiffness”  $\rho_s$  decreases monotonically with increasing measurement strength,  $\gamma$ , it is natural to expect that the charge-sharpening transition in 1+1d is a Kosterlitz-Thouless (KT)-type transition where vortex-proliferation destroys the IRSF QLRO for  $p > p_\#$ , i.e.  $\gamma > \gamma_\#$ , resulting in a “Mott insulating” phase. This picture will turn out to be qualitatively correct, albeit with important quantitative changes to the usual KT transition due to the replica structure.

**Charge-sharpening in 1+1d** – To obtain a controlled theory of the transition, we introduce vortex defects into Eq. 4 by standard duality methods [72] to obtain modified “sine-Gordon” model:

$$\mathcal{L}_{\text{dual}} = \frac{1}{8\pi^2\bar{\rho}} \left[ (\partial_t \bar{\vartheta})^2 + D^2 (\partial_x^2 \bar{\vartheta})^2 \right] + \frac{1}{8\pi^2\rho_s} (\Pi \partial_\mu \vartheta)^2 - \lambda \sum_{a \neq b} \cos(\vartheta_a - \vartheta_b), \quad (5)$$

where  $D \sim J$ ,  $e^{-i\vartheta_a}$  inserts a (spacetime/instanton) vortex, and  $\vartheta$  are related to the original fields by  $\rho_s \partial_\mu \phi_a \leftrightarrow \frac{\epsilon^{\mu\nu}}{2\pi} \partial_\nu \vartheta_a$ ,  $\lambda \approx e^{-\sqrt{J/\gamma}}$  is the vortex fugacity, and we have kept only the most relevant vortex terms. Note that the minimal topological defects that can appear are actually a bound states of a vortex and anti-vortex in different replicas. Formally, this is because individual vortices, which contribute vorticity to  $\bar{\phi}$ , are linearly confined by the diffusive replica-average mode. Intuitively, this simply reflects the absence of quantum fluctuations in the Heisenberg ferromagnet ground-state that describes

replica-averages in the steady-state. An immediate consequence of this vortex-“doubling” is that it *halves* the critical superfluid stiffness compared to the ordinary KT transition:  $(\rho_s)_\# = \pi^{-1} = \frac{1}{2} (\rho_s)_{\text{KT}}$ . We further note, that in an ordinary superfluid, vortex condensation requires commensuration between particle density and the lattice, otherwise vortex instantons acquire non-trivial Berry phases and are suppressed. Here, the density conjugate to the composite vortex operators are inter-replica density fluctuations, which has vanishing average independent of the physical (replica-average) charge density. Consequently, in 1+1d, there is a single universality class for charge-sharpening, in contrast to the ordinary superfluid-Mott transition which arises only at integer densities and exhibits different scalings in the presence or absence of particle-hole symmetry.

**Observables and numerics** – In 1+1d, the fuzzy-phase/IRSF exhibits only quasi-long-range order (QLRO), with algebraic decay of charge ( $\sigma^z \approx \frac{1}{\pi} \partial_x \vartheta$ ) correlators,  $C_z(x) = \mathbb{E}[\langle \sigma^z(x) \sigma^z(0) \rangle - \langle \sigma^z(x) \rangle \langle \sigma^z(0) \rangle]$ , which are negative at large distance in the steady state. This changes to short-range correlations in the gapped phase:

$$C_z(x) \sim - \begin{cases} \rho_s (a/x)^{-2} & p \leq p_\# \\ e^{-x/\xi} & p > p_\# \end{cases} + \dots \quad (6)$$

where  $a$  is a non-universal UV cutoff (lattice spacing),  $\xi$  is a finite correlation length and  $(\dots)$  denote asymptotically subleading terms. This behavior is consistent in TEBD results for the discrete-time model Eq. 1 showing an algebraic decay of  $\mathbb{E}[\langle \sigma^z(x) \sigma^z(0) \rangle_c]$  with power-law fit that is constant over an extended range  $0 < p < p_\# \approx 0.2$  (Fig. 2a,c).

A hallmark of KT-physics is that certain correlators exhibit continuously evolving critical exponents in the QLRO Goldstone-phase. Constraining ourselves to charge-diagonal quantities that can be physically

probed in the original qubit language, a convenient observable that displays this behavior are the string operators:  $W_{[0,x]} = e^{-i\pi \sum_{i \in (0,x)} \sigma_i^z / 2} \approx e^{-i\frac{1}{2} \int_0^x d\vartheta} = e^{-i\vartheta(x)/2} e^{i\vartheta(0)/2}$ , which inserts a  $\pi$ -phase twist in the  $\phi$ -fields in the interval  $[0, x]$ , and can be thought of as a dual (boundary) order parameter for vortex condensation:

$$C_W(x) = \mathbb{E} [\langle W_{[0,x]} \rangle^2] \approx \begin{cases} |x|^{-2\pi\rho_s} & p \leq p_{\#} \\ \text{constant} & p > p_{\#} \end{cases}. \quad (7)$$

The scaling dimension of  $W$  decreases monotonically with measurement rate  $\gamma$  (as  $\sim \gamma^{-1/2}$  for small  $\gamma$ ), and jumps (for  $L \rightarrow \infty$ ) discontinuously to 0 in the charge-sharp phase ( $\gamma > \gamma_{\#}$ ), achieving a minimum non-zero value of  $\Delta_W = 1$  at the sharpening transition ( $\gamma = \gamma_{\#}$ ).

The predicted power-law decay of charge- and string-correlators are in excellent agreement with TEBD data (Fig. 2) for  $0 < p \leq p_{\#} \approx 0.2$ . We note that, as is typical for two-parameter scaling KT-transitions, incorrectly applying a single-parameter scaling analysis with finite correlation-length exponent,  $\nu$  as in Ref. [56] dramatically overestimates the critical measurement strength, and misses the key physics of continuously evolving scaling exponents in the charge-fuzzy phase.

**Discussion** – The agreement with unbiased numerics gives strong support to the hypothesis that the continuum field theory description captures the universality class of charge sharpening in the discrete-time, strong-measurement model. Importantly, the analytic replica field theory approach can be applied in more complicated scenarios where numerics becomes challenging. In the supplemental material [72], we give a general argument that the charge-sharpening transition occurs separately from, and precedes the entanglement transition in any spatial dimension  $D$ , and show that for  $U(1)$ -symmetry is again described by  $(Q-1)$  coupled XY-models for the inter-replica modes. A new feature of  $D \geq 2$   $U(1)$ -MRCs is that, since circuit-evolution time plays the role of temperature in the stat-mech model, for  $p < p_{\#}$ , the system exhibits a finite-time transition at critical time  $t_c$ , where the long-range correlations appear, although the charge remains “fuzzy” until a time  $\sim L^D$ . For  $D \geq 2$  this finite-time transition has the same critical properties as a superfluid transition at nonzero temperature in  $D$  dimensions. This critical time diverges as  $t_c \sim |p - p_{\#}|^{-z/\nu}$  with  $z = 1$  and  $\nu = \nu_{D+1}$ . Evidence and arguments for related finite-time complexity [67] and entanglement [73] transitions in MRCs have previously been discussed absent symmetries, however, in the present case, the field theory approach gives a controlled calculation of critical properties in generic Haar-random circuit models. A second twist that arises in  $D \geq 2$  is the emergence of multiple classes of boundary-criticality governing the steady-state behavior of MRCs: i) ordinary (bulk or-

ders before boundary), ii) extra-ordinary (boundary orders before bulk), and iii) special (boundary transition between ordinary and extraordinary), depending on the relative bulk and boundary coupling strengths. Here, the extra-ordinary to ordinary boundary transition can be tuned by increasing the number of measurements in the final few circuit layers compared to the bulk. The properties of the extraordinary transition for the  $2+1d$  XY model were worked out only very recently [74], and exhibits an unusual log-divergence of  $\rho_s$  upon approaching the bulk phase transition with the QLRO surface. A third new feature that arises in  $2+1d$  and  $3+1d$  when we move away for mean charge density zero is a relevant coupling between the charge diffusion and the inter-replica dynamics via the dependence of  $\rho_s$  on the local charge density, which moves the sharpening transition to a new universality class with quenched disorder and, presumably,  $z > 1$ .

It is straightforward to generalize the field theory approach to study charge-sharpening transitions with discrete symmetries. The main difference compared to continuous symmetry is the absence of gapless Goldstone modes in the discrete-charge-fuzzy phase, so that correlators are either long-range or exponential decaying. By way of standard duality transformations [56, 75], the existence of discrete charge-sharpening implies the existence of sharp symmetry-breaking and topological-ordering/(de)confinement transitions *within the volume law entangled regime* whereas only classical orders would be allowed in thermal equilibrium. The prospect of a quantum-ordered phases in volume-law entangled trajectories was discussed in various Clifford models [52]. Our field-theory technique not only places this discussion on firmer ground for generic (Haar-random) MRC classes, but also enables controlled calculation of symmetry-breaking and topological MITs.

Finally, we expect that our approach can be readily adapted to study a wide variety of measurement induced phenomena arising in monitored random circuits such as those with more complicated (e.g. non-Abelian) symmetries, competing types of non-commuting measurements, and fracton-like kinetic constraints such as dipole- and higher-multipole conservation or subsystem symmetries [76, 77].

*Acknowledgements* – We thank A. Zabalo, K. Chen, M.P.A. Fisher, M. Gullans, J. Pixley and J. Wilson for useful discussions and/or earlier collaborations on charge sharpening transitions. The tensor network simulations are based on the quimb library [78]. We acknowledge support from NSF DMR-1653271 (S.G.), NSF DMR-1653007 (A.C.P.), NSF QLCI grant OMA-2120757 (D.A.H.), the Air Force Office of Scientific Research under Grant No. FA9550-21-1-0123 (F.B. and R.V.), and the Alfred P. Sloan Foundation through Sloan Research Fellowships (A.C.P. and R.V.).

- 
- [1] P. Hayden and J. Preskill, **2007**, 120 (2007).
- [2] Y. Sekino and L. Susskind, **2008**, 065 (2008).
- [3] W. Brown and O. Fawzi, *Communications in Mathematical Physics* **340**, 867 (2015).
- [4] P. Hosur, X.-L. Qi, D. A. Roberts, and B. Yoshida, *Journal of High Energy Physics* **2016**, 4 (2016).
- [5] R. Oliveira, O. C. O. Dahlsten, and M. B. Plenio, *Phys. Rev. Lett.* **98**, 130502 (2007).
- [6] F. G. S. L. Brandão, A. W. Harrow, and M. Horodecki, *Communications in Mathematical Physics* **346**, 397 (2016).
- [7] A. Nahum, J. Ruhman, S. Vijay, and J. Haah, *Phys. Rev. X* **7**, 031016 (2017).
- [8] A. Nahum, S. Vijay, and J. Haah, *Physical Review X* **8** (2018), 10.1103/PhysRevX.8.021014, arXiv:1705.08975.
- [9] B. Bertini, P. Kos, and T. c. v. Prosen, *Phys. Rev. X* **9**, 021033 (2019).
- [10] C. W. Von Keyserlingk, T. Rakovszky, F. Pollmann, and S. L. Sondhi, *Physical Review X* **8** (2018), 10.1103/PhysRevX.8.021013, arXiv:1705.08910.
- [11] V. Khemani, A. Vishwanath, and D. A. Huse, *Phys. Rev. X* **8**, 031057 (2018).
- [12] T. Rakovszky, F. Pollmann, and C. W. von Keyserlingk, *Phys. Rev. X* **8**, 031058 (2018).
- [13] A. Chan, A. De Luca, and J. T. Chalker, *Phys. Rev. X* **8**, 041019 (2018).
- [14] B. Bertini, P. Kos, and T. c. v. Prosen, *Phys. Rev. Lett.* **121**, 264101 (2018).
- [15] A. Chan, A. De Luca, and J. T. Chalker, *Phys. Rev. Lett.* **121**, 060601 (2018).
- [16] A. J. Friedman, A. Chan, A. De Luca, and J. T. Chalker, *Physical Review Letters* **123**, 210603 (2019), arXiv:1906.07736.
- [17] S. Gopalakrishnan and A. Lamacraft, *Phys. Rev. B* **100**, 064309 (2019).
- [18] B. Bertini, P. Kos, and T. c. v. Prosen, *Phys. Rev. Lett.* **123**, 210601 (2019).
- [19] Y. Li, X. Chen, and M. P. A. Fisher, *Phys. Rev. B* **98**, 205136 (2018).
- [20] B. Skinner, J. Ruhman, and A. Nahum, *Physical Review X* **9** (2019), 10.1103/PhysRevX.9.031009, arXiv:1808.05953.
- [21] Y. Li, X. Chen, and M. P. Fisher, *Physical Review B* **100**, 134306 (2019), arXiv:1901.08092.
- [22] A. Chan, R. M. Nandkishore, M. Pretko, and G. Smith, *Phys. Rev. B* **99**, 224307 (2019).
- [23] Y. Li, X. Chen, A. W. W. Ludwig, and M. P. A. Fisher, arXiv:2003.12721 [cond-mat, physics:quant-ph] (2020), arXiv:2003.12721.
- [24] X. Cao, A. Tilloy, and A. D. Luca, *SciPost Phys.* **7**, 24 (2019).
- [25] M. J. Gullans and D. A. Huse, *Phys. Rev. X* **10**, 041020 (2020).
- [26] M. Szyniszewski, A. Romito, and H. Schomerus, *Physical Review B* **100** (2019), 10.1103/PhysRevB.100.064204, arXiv:1903.05452.
- [27] S. Choi, Y. Bao, X. L. Qi, and E. Altman, *Physical Review Letters* **125** (2020), 10.1103/PhysRevLett.125.030505, arXiv:1903.05124.
- [28] Y. Bao, S. Choi, and E. Altman, *Physical Review B* **101** (2020), 10.1103/PhysRevB.101.104301, arXiv:1908.04305.
- [29] C. M. Jian, Y. Z. You, R. Vasseur, and A. W. Ludwig, *Physical Review B* **101** (2020), 10.1103/PhysRevB.101.104302, arXiv:1908.08051.
- [30] M. J. Gullans and D. A. Huse, *Physical Review Letters* **125** (2020), 10.1103/PhysRevLett.125.070606, arXiv:1910.00020.
- [31] A. Zabalo, M. J. Gullans, J. H. Wilson, S. Gopalakrishnan, D. A. Huse, and J. H. Pixley, *Physical Review B* **101** (2020), 10.1103/PhysRevB.101.060301, arXiv:1911.00008.
- [32] A. Nahum and B. Skinner, *Phys. Rev. Research* **2**, 023288 (2020).
- [33] M. Ippoliti, M. J. Gullans, S. Gopalakrishnan, D. A. Huse, and V. Khemani, (2020), arXiv:2004.09560.
- [34] A. Lavasani, Y. Alavirad, and M. Barkeshli, (2020), arXiv:2004.07243.
- [35] S. Sang and T. H. Hsieh, arXiv:2004.09509 [cond-mat, physics:quant-ph] (2020), arXiv:2004.09509.
- [36] Q. Tang and W. Zhu, *Phys. Rev. Research* **2**, 013022 (2020).
- [37] J. Lopez-Piqueres, B. Ware, and R. Vasseur, *Phys. Rev. B* **102**, 064202 (2020).
- [38] A. Nahum, S. Roy, B. Skinner, and J. Ruhman, *PRX Quantum* **2**, 010352 (2021).
- [39] X. Turkeshi, R. Fazio, and M. Dalmonte, *Physical Review B* **102** (2020), 10.1103/PhysRevB.102.014315, arXiv:2007.02970.
- [40] Y. Fuji and Y. Ashida, arXiv:2004.11957 [cond-mat, physics:quant-ph] (2020), arXiv:2004.11957.
- [41] O. Lunt, M. Szyniszewski, and A. Pal, *Dimensional hybridity in measurement-induced criticality*, Tech. Rep., arXiv:2012.03857v1.
- [42] O. Lunt and A. Pal, (2020), arXiv:2005.13603.
- [43] R. Fan, S. Vijay, A. Vishwanath, and Y.-Z. You, arXiv:2002.12385 [cond-mat, physics:quant-ph] (2020), arXiv:2002.12385.
- [44] S. Vijay, arXiv e-prints, arXiv:2005.03052 (2020), arXiv:2005.03052 [quant-ph].
- [45] Y. Li and M. P. A. Fisher, (2020), arXiv:2007.03822.
- [46] X. Turkeshi, A. Biella, R. Fazio, M. Dalmonte, and M. Schiró, *Phys. Rev. B* **103**, 224210 (2021).
- [47] M. Ippoliti and V. Khemani, *Phys. Rev. Lett.* **126**, 060501 (2021).
- [48] T.-C. Lu and T. Grover, arXiv e-prints, arXiv:2103.06356 (2021), arXiv:2103.06356 [quant-ph].
- [49] C.-M. Jian, B. Bauer, A. Keselman, and A. W. W. Ludwig, arXiv e-prints, arXiv:2012.04666 (2020), arXiv:2012.04666 [cond-mat.stat-mech].
- [50] S. Gopalakrishnan and M. J. Gullans, *Phys. Rev. Lett.* **126**, 170503 (2021).
- [51] X. Turkeshi, arXiv e-prints, arXiv:2101.06245 (2021), arXiv:2101.06245 [cond-mat.stat-mech].
- [52] Y. Bao, S. Choi, and E. Altman, arXiv e-prints, arXiv:2102.09164 (2021), arXiv:2102.09164 [cond-mat.stat-mech].
- [53] M. Block, Y. Bao, S. Choi, E. Altman, and N. Yao, arXiv e-prints, arXiv:2104.13372 (2021), arXiv:2104.13372 [quant-ph].
- [54] G. Bentsen, S. Sahu, and B. Swingle, arXiv e-prints,

- arXiv:2104.07688 (2021), arXiv:2104.07688 [quant-ph].
- [55] A. Zabalo, M. J. Gullans, J. H. Wilson, R. Vasseur, A. W. W. Ludwig, S. Gopalakrishnan, D. A. Huse, and J. H. Pixley, arXiv e-prints , arXiv:2107.03393 (2021), arXiv:2107.03393 [cond-mat.dis-nn].
- [56] U. Agrawal, A. Zabalo, K. Chen, J. H. Wilson, A. C. Potter, J. H. Pixley, S. Gopalakrishnan, and R. Vasseur, arXiv e-prints , arXiv:2107.10279 (2021), arXiv:2107.10279 [cond-mat.dis-nn].
- [57] Y. Li and M. P. A. Fisher, arXiv e-prints , arXiv:2108.04274 (2021), arXiv:2108.04274 [quant-ph].
- [58] O. Alberton, M. Buchhold, and S. Diehl, Phys. Rev. Lett. **126**, 170602 (2021).
- [59] S.-K. Jian, C. Liu, X. Chen, B. Swingle, and P. Zhang, arXiv e-prints , arXiv:2106.09635 (2021), arXiv:2106.09635 [quant-ph].
- [60] O. Lunt, M. Szyniszewski, and A. Pal, arXiv e-prints , arXiv:2012.03857 (2020), arXiv:2012.03857 [quant-ph].
- [61] M. Buchhold, Y. Minoguchi, A. Altland, and S. Diehl, arXiv e-prints , arXiv:2102.08381 (2021), arXiv:2102.08381 [cond-mat.stat-mech].
- [62] X. Turkeshi, M. Dalmonte, R. Fazio, and M. Schirò, “Entanglement transitions from stochastic resetting of non-hermitian quasiparticles,” (2021), arXiv:2111.03500 [cond-mat.stat-mech].
- [63] R. Vasseur, A. C. Potter, Y.-Z. You, and A. W. W. Ludwig, Phys. Rev. B **100**, 134203 (2019).
- [64] T. Zhou and A. Nahum, Physical Review B **99** (2019), 10.1103/PhysRevB.99.174205, arXiv:1804.09737.
- [65] M. J. Gullans, S. Krastanov, D. A. Huse, L. Jiang, and S. T. Flammia, Phys. Rev. X **11**, 031066 (2021).
- [66] N. Hunter-Jones, arXiv e-prints , arXiv:1905.12053 (2019), arXiv:1905.12053 [quant-ph].
- [67] J. Napp, R. L. La Placa, A. M. Dalzell, F. G. S. L. Brandao, and A. W. Harrow, (2019), arXiv:2001.00021.
- [68] C. Noel, P. Niroula, D. Zhu, A. Risinger, L. Egan, D. Biswas, M. Cetina, A. V. Gorshkov, M. J. Gullans, D. A. Huse, and C. Monroe, arXiv e-prints , arXiv:2106.05881 (2021), arXiv:2106.05881 [quant-ph].
- [69] G. Vidal, Phys. Rev. Lett. **91**, 147902 (2003).
- [70] G. Vidal, Phys. Rev. Lett. **93**, 040502 (2004).
- [71] U. Schollwöck, Annals of Physics **326**, 96 (2011), january 2011 Special Issue.
- [72] See supplemental information for details of derivation of effective field theory and numerical methods..
- [73] Y. Bao, M. Block, and E. Altman, arXiv e-prints , arXiv:2110.06963 (2021), arXiv:2110.06963 [quant-ph].
- [74] M. A. Metlitski, arXiv e-prints , arXiv:2009.05119 (2020), arXiv:2009.05119 [cond-mat.str-el].
- [75] M. Fisher, in *Strong interactions in low dimensions* (Springer, 2004) pp. 419–438.
- [76] E. Guardado-Sanchez, A. Morningstar, B. M. Spar, P. T. Brown, D. A. Huse, and W. S. Bakr, Physical Review X **10**, 011042 (2020).
- [77] A. Gromov, A. Lucas, and R. M. Nandkishore, Physical Review Research **2**, 033124 (2020).
- [78] J. Gray, Journal of Open Source Software **3**, 819 (2018).
- [79] A. B. Harris, **7**, 1671 (1974).